1 NOMENCLATURE

Roman

A	cross-sectional area
c	specific heat
d	differential
f_v	volumetric void fraction
G	Gibbs free energy
g	specific free energy
H	enthalpy
h	specific enthalpy
k	thermal conductivity
ℓ	length
M	mass in V
m	mass
Q	heat
q	heat
R	molar gas constant
R^*	specific gas constant
S	entropy
s	specific entropy
T	temperature
t	time
u	velocity
V	volume
v	specific volume
W	work
X	generic variable
x	specific generic variable
x	molar fraction
y	displacement
Z	compression factor
z	displacement

Greek/Math

∂	partial derivative
∇	gradient
β	expansivity
γ	specific heat ratio c_P/c_V
δ	deviation
Δ	difference
ε	effectiveness
η	efficiency
η	enthalpy perturbation
λ	thermal penetration depth
μ	chemical potential
μ	mass perturbation
Π	dimensionless pressure
σ	entropy perturbation
τ	oscillation period
τ	temperture perturbation
φ	phase
ω	frequency [radians/s]

Superscript

$\dot{}$	flow
$\bar{}$	mean
g	gas
gw	gas to wall
w	wall

Subscript

3	^{3}He
4	^{4}He
a	average (mean)
c	cold heat exchanger
d	dynamic (amplitude)
dc	dc
eff	effective
ex	heat exchanger
excess	excess
gas	gas
gen	generation
H	enthalpy
h	hot heat exchanger
i	index
i	ideal
in	inlet
int	internal
inv	inversion
k	thermal conduction
loss	loss
m	mass
min	minimum
o	aftercooler
out	outlet
P	pressure
pt	pulse tube
real	real (actual)
regen	regenerator
S	entropy
solid	solid
T	temperature
total	total
V	volume
x	generic variable
Δ	ΔT

8 APPENDICES

A Heat Transfer Losses in Basic Pulse Tube

As was shown in Sec. 4.11, the ideal BPTR produced no cooling. This is a result of the mass flow being adiabatic and out of phase with the pressure and temperature oscillations. In practice, the BPTR does produce a small amount of cooling, the result of heat transfer between the pulse tube wall and the gas. Various methods of calculating the performance of BPTRs have been given elsewhere.[65] Here, a method based on heat transfer in the pulse tube boundary layer will be discussed.

If we assume that the gas to wall interaction results in small perturbations in h, s, T, and $\dot{m}$:

$$h = h_i + \eta \ , \ s = s_i + \sigma \ , \ T = T_i + \tau \ , \text{ and } \dot{m} = \dot{m}_i + \dot{\mu} \ , \tag{A1}$$

where dh, ds, and dg are given by (3.5 – 3.7) respectively and the perturbations are assumed to be small ($|\eta| \ll |h_i|$, $|\tau| \ll |T_i|$, and $|\mu| \ll |\dot{m}_i|$) and out of phase with the ideal quantities. Only the oscillating portions of h, s, T, and $\dot{m}$ contribute to the cyclic averages. Therefore, only the oscillating terms need to be included in (A1). Then, by (4.13) and (4.29):

$$\frac{1}{\tau}\oint_0^\tau \dot{m}_i h_i dt = 0, \ \frac{1}{\tau}\oint_0^\tau \dot{\mu}\eta dt = 0, \text{ and } s_i = 0. \tag{A2}$$

The perturbations yield small enthalpy and entropy flows:

$$\dot{H} = \frac{1}{\tau}\oint_0^\tau \dot{m} h dt \approx \frac{1}{\tau}\oint_0^\tau \dot{\mu} h_i dt + \frac{1}{\tau}\oint_0^\tau \dot{m}_i \eta dt, \tag{A3}$$

$$\dot{S} = \frac{1}{\tau}\oint_0^\tau \dot{m} s dt \approx \frac{1}{\tau}\oint_0^\tau \dot{m}_i \sigma dt, \tag{A4}$$

and

$$\dot{G} = \dot{H} - T\dot{S} \tag{A5}$$

which result in cooling at the cold heat exchanger and dissipation at the hot heat exchanger.

One can estimate the size of the perturbations from a simple model of the BPTR pulse tube. Consider approximating the motion of an element of gas in the pulse tube as a four-step cycle. In this approximation, the gas element moves toward the hot heat exchanger as it is compressed adiabatically. The element pauses briefly at its maximum displacement. It then retraces its path expanding adiabatically. Finally, it pauses at its initial starting point. In a real basic pulse tube, there is some heat transfer between the walls and our gas element. Assume this occurs only during the pauses and that the pauses are isobaric. Now, as heat is transferred at the first pause, the gas cools and continues to move toward the hot heat exchanger. Similarly, at the second pause, the gas warms and continues to move toward the cold heat exchanger. Since the heat transfer only occurs for a short time, only the gas within the thermal penetration depth is cooled or warmed, respectively.

In analyzing this cycle we will assume small amplitude variations about mean values and that the wall temperature is steady and equal to the local mean gas temperature, $T_a^w(z) = T_a^g(z)$. During the adiabatic legs, an element of gas is displaced a distance y_d, where $v = yA$ is the

volume between the gas element and the hot heat exchanger. This definition of y results in $dz = -dy$. Then from (5.16):

$$y_d = \frac{P_d}{P_a}\frac{v_a}{\gamma A}. \tag{A6}$$

After the compression, the heated and displaced gas element ends at a section of wall that is also hotter than the starting point. The temperature difference between the gas and the wall becomes:

$$\Delta T_d^{gw} = \left.\frac{\partial T^g}{\partial P}\right|_S P_d - \frac{\partial T^w}{\partial z}\frac{dz}{dy}y_d \tag{A7}$$

or

$$\Delta T_d^{gw} = \frac{P_d}{P_a}\left[T^w\left(1 - \frac{1}{\gamma}\right) - \frac{v_a}{\gamma A}\frac{\partial T^w}{\partial z}\right]. \tag{A8}$$

During the isobaric leg, the gas within the thermal penetration depth, λ, cools to the local T^w and the mean gas temperature changes by

$$\tau \approx \frac{2\lambda}{r}\Delta T^{gw} \tag{A9}$$

where $2\lambda/r$ is the ratio of the volume of the thermal penetration layer to the volume of the gas element. The enthalpy perturbation is $\eta = c_P\tau$. Combining the two isobaric legs, there is no net heat flow between the gas and the wall. During the cooling leg, there is an additional displacement, δy_d, which can be found by $\partial v/\partial T|_P$ for an ideal gas:

$$\delta y_d = \frac{v_d\tau}{AT^w}. \tag{A10}$$

The mass flows are proportional to the displacements. Thus,

$$\dot{\mu} = \frac{\delta y_d}{y_d}\dot{m}_d. \tag{A11}$$

One can now combine (A3-A11) to calculate the mass flow and temperature perturbations and from those the enthalpy and entropy flows. Instead, we will find the phase shifts from these perturbations. The perturbations shift the phase of $\dot{m}$ and T by

$$\varphi_m = \frac{\delta y_d}{y_d} \text{ and } \varphi_T = \frac{\tau_d}{T_d}. \tag{A12}$$

These can be evaluated at the cold heat exchanger, yielding

$$\varphi_m \approx -(\gamma - 1)\varphi_T \tag{A13}$$

and

$$\varphi_T \approx \frac{2\lambda}{r}\left[1 - \frac{1}{\gamma - 1}\left(\frac{T_h - T_c}{T_c}\right)\right]. \tag{A14}$$

where the temperature gradient was approximated by the mean temperature gradient.

The total phase shift, $\varphi_{mT} = \varphi_m - \varphi_T = -\gamma\varphi_T$, is small. The factor γ is the result of the assumed path of the secondary compression. These phase shifts result in a small enthalpy flow:

$$\dot{H} \approx \frac{\gamma}{\tau}\int_0^{\tau}\dot{m}_i\eta\,dt \approx \frac{\gamma\varphi_T}{2}\dot{m}_d c_P T_d^g \approx \frac{(\gamma - 1)}{2}\varphi_T\dot{m}_d c_P T_a^w\frac{P_d}{P_a}. \tag{A15}$$

Since $\dot{m}_d T_a^w$ is constant along the pulse tube (4.14) and φ_T is roughly constant (A14), $\dot{H}$ is approximately constant.

When φ_T in (A14) is 0, the enthalpy flow ≈ 0. This defines the minimum temperature a BPTR can reach:

$$T_{c\min} \approx T_h/\gamma\ . \tag{A16}$$

For T_h = 280 K, $T_{c\ min} \approx$ 168 K for helium and $T_{c\ min} \approx$ 200 K for air. Eq. (A16) is based on a simplification of the heat transfer process and can only be considered approximation of the true limit. Yet, a survey[66] (summarized in Table A1) of BPTRs found that most had T_c above or near the minimum. The lowest temperature reached was 135 K in a large amplitude (P_d/P_a = 0.6) helium PTR.[67]

Table A1: Summary of an early survey of BPTR minimum temperatures.[66]

Reference	Gas	Hot Ht. Ex. Temp. (K)	Cold Ht. Ex. Temp. (K)	Cold Load (W)
68	air	303	214.5	0
69	He	293	169	0
69	He	293	177	0
69	He	293	181	0
69	He	293	230	0
70	He		163	0
71	He	290	150	0
72	He		185	0
72	He		160	0
72	He		135	0
73	He		185	0
73	He		160	0
74	He	294	167	0
75	He	289	165	0
76	He	283	169	0
76	He	282	167	0

The analysis here only includes heat transfer near the minimum and maximum displacements. When heat transfer over the whole cycle is included, a more complete calculation found that the minimum temperature could be lower than T_h/γ.[65]

The heat transfer induced phase shift results in entropy generation. By (5.1) this is

$$\nabla \frac{dS_{gen}}{dt} = \nabla \dot{q} \frac{\Delta T}{T_w^2}, \tag{A17}$$

where

$$\nabla \dot{q} = \frac{2\lambda}{r} \nabla M c_P \Delta T \tag{A18}$$

is the heat needed to change the mass within the thermal penetration depth by ΔT. Thus $S_{gen} \propto (\Delta T/T_w)^2$. It is a second order term and can be ignored. By (3.23), the entropy flow is also small.

B Pulse Tube to Heat Exchanger Transition

The transition between an isothermal heat exchanger ($\dot{H} = 0$) and the adiabatic pulse tube ($\dot{S} = 0$) will be discussed here. At these transitions (Figure 4), the enthalpy flow in the pulse tube vanishes. Two-dimensional modeling using a commercial computational fluid dynamics, CFD, application has shown that in this region there are four types of temperature profiles during each cycle.[51] These are shown in Figure B1 for the transition at the hot heat exchanger. The figures would be inverted for the cold transition. The figures show two types of processes:

1) One type occurs when the mass flow is from the heat exchanger and into the pulse tube: (d) and (a) in Figure B1. The flow leaves the heat exchanger at the temperature of the heat exchanger with no convective heat transfer. Once in the pulse tube, the changing pressure causes the gas temperature to change. This results in a temperature gradient in the pulse tube and thermal conduction between the gas in the pulse tube and the heat exchanger. This process is described by (4.42).
2) The other type occurs when the gas flows from the pulse tube and into the heat exchanger: (b) and (c) in Figure B1. The gas enters the heat exchanger and its temperature rapidly changes to equilibrate with the heat exchanger. The temperature gradient is very much greater than in the previous case. Thus, much more heat is transferred. The heat transferred is

$$\dot{Q} = \dot{m} c_P \Delta T, \tag{B1}$$

where ΔT is the temperature change of the gas on entering the heat exchanger. This convective heat transfer tracks the gas temperature near the heat exchanger.

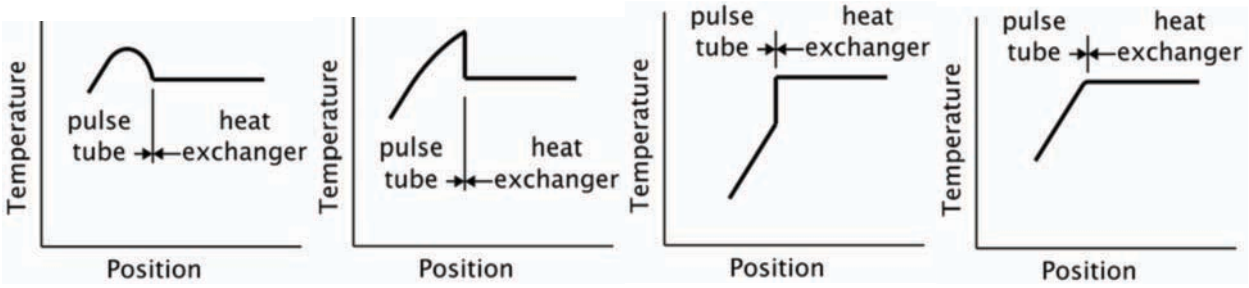

Figure B1: The temperature profile at the pulse tube/hot heat exchanger interface in a PTR with inertance tube is illustrated in sequence during the cycle. The pressure is above the mean pressure in (a) and (b) and below the mean pressure in (c) and (d). The mass flow is from the heat exchanger into the pulse tube in (a) and (d) and is reversed in (b) and (c).

The sequence shown in Figure B1 are for an IPTR. The sequence is reversed for an OPTR. The heat transfer for both configurations is illustrated in Figure B2. The illustrations combine both conduction and convection. The illustrated amplitudes of the two terms are arbitrary. The phase shifts between the mass flow and pressure used in Figure B2 are given in Table B1 and were chosen to be near optimal for each configuration.[62] The path followed by gas elements in the transition region for several different cycles has been discussed elsewhere.[32]

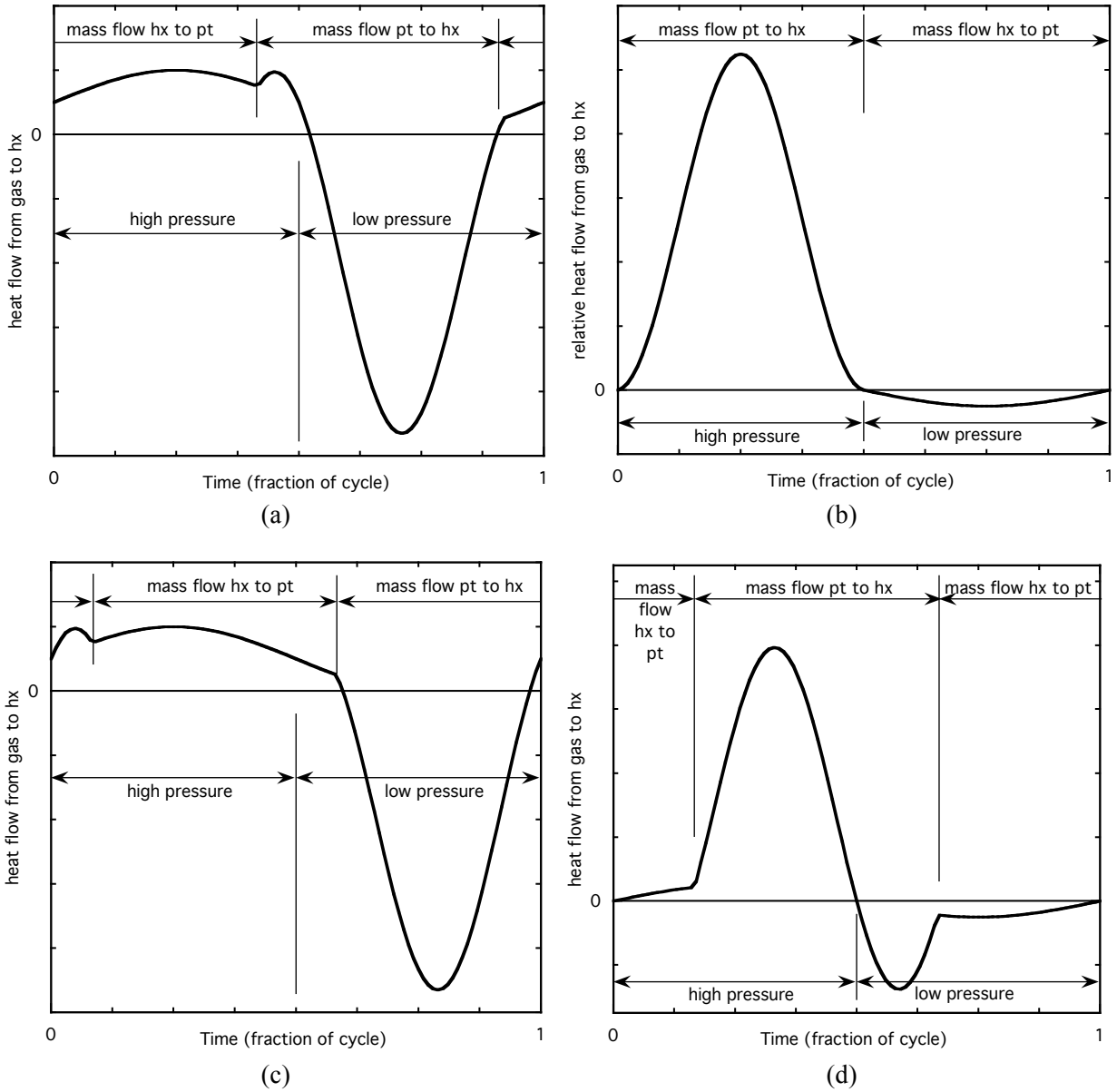

Figure B2: Qualitative representations of the heat flow from the working fluid (gas) to the heat exchangers for an orifice pulse tube cooler (a, b) and an inertance tube pulse tube cooler (c, d). The transition at the cold heat exchanger (a, c) and the hot heat exchanger (b, d) are shown. The regions of $P > P_0$ and $P < P_0$ are indicated, as are the regions where the mass flows from the pulse tube (pt) to the heat exchanger (hx) and vice versa.

Table B1: Phase shift used in Fig. 4 between mass flow and pressure (mass flow lag < 0, lead > 0)

Type of Pulse Tube Cooler	at Cold Heat Exchanger	at Hot Heat Exchanger
Orifice	30°	0°
Inertance Tube	-30°	-60°

The heat transfer is not a simple function expressible in the form assumed in the small amplitude approximation, (3.2 – 3.3). The conduction term can be approximated by (3.2 – 3.3). The convection term only lasts half a cycle. It is of the form:

for $\dot{m}$ into heat exchanger $$\dot{Q} = \dot{q}_0 + \dot{q}_1 \sin\left(2\omega t + \varphi\right) \tag{B2}$$

and for $\dot{m}$ out of heat exchanger $$\dot{Q} = 0, \tag{B3}$$

where $\dot{q}_0$, $\dot{q}_1$, and φ are interdependent constants with the constraint that $\dot{Q}$ is continuous. The convection term represents the conversion between the enthalpy flow in the pulse tube and heat exchanged to the heat exchanger. Thus, there is a transition region near the heat exchanger where there is a transition from pure enthalpy flow of the form of (3.2 – 3.3) to the form of (B2 – B3). This transition region is of the order of the distance a gas element penetrates the pulse tube during a cycle. Evidence of this transition may have been seen in temperature measurements in the transfer line between a compressor and a regenerator.[77]

Because of the asymmetry in (B2 – B3), there is a net heat flow between the gas and the heat exchanger and the mean gas temperature near the end of the pulse tube differs from the heat exchanger's temperature. The contribution to the heat transfer from the convection term is $\dot{q}_0/2$. Conduction decreases the heat transfer and temperature offset at both heat exchangers. The mean temperature offsets increases the heat conducted in the central region of the pulse tube. The entropy generative in the process discussed earlier (Sec. 5.6) assumed that ΔT is constant over a cycle. A more precise calculation is given by integrating (5.1) over a cycle:

$$\bar{S}_{gen} = T_{ex}^{-2} \frac{1}{\tau} \oint_0^\tau \dot{Q} \Delta T \, d\tau. \tag{B4}$$

where T_{ex} is the heat exchanger temperature.

C ^{3}He Quasi Particles in Superfluid ^{4}He

The previous discussion (Sec. 7) on the minimum temperature of a PTR assumes that the mixture moves as a bulk fluid. In the superfluid region, He-II, the fluid can act as two interpenetrating fluids, which can move independently. One is the pure ^{4}He superfluid component. The other is the normal fluid component consisting of some ^{4}He and all of the ^{3}He. Near the λ-line, most of the fluid is in the normal state. Below ≈ 1 K, the normal fluid consists of only ^{3}He quasi particles. If the piston in the compressor has a superleak, then the ^{3}He can act as a low-density gas moving in a fixed ^{4}He background. A full treatment of the thermodynamics in this regime is beyond the scope of this paper. Reviews of the thermodynamics of dilute ^{3}He in ^{4}He solutions have been given elsewhere.[78,79,80]

A PTR using dilute ^{3}He in a fixed ^{4}He background was developed at Los Alamos. It operated between 1 K and 0.6 K.[81] The system pressure is fixed by the conditions in the compressor/aftercooler. The compressor does not cause pressure oscillations; rather it causes the ^{3}He concentration, x_3, and the osmotic pressure, Π_3, to oscillate. Pressure gradients in the regenerator, heat exchangers, and orifices are replaced by gradients in Π_3. In the pulse tube, the constraint that $\nabla P = 0$ is replaced by $\nabla\mu_4 = 0$, where μ_4 is the chemical potential of the ^{4}He. Several loci of $\nabla\mu_4 = 0$ are shown in Figure C1. For constant μ_4, x_3 increases as the temperature decreases. The cold end temperature is limited by phase separation. The Los Alamos PTR was filled with $x_3 = 0.17$ before being turned on.

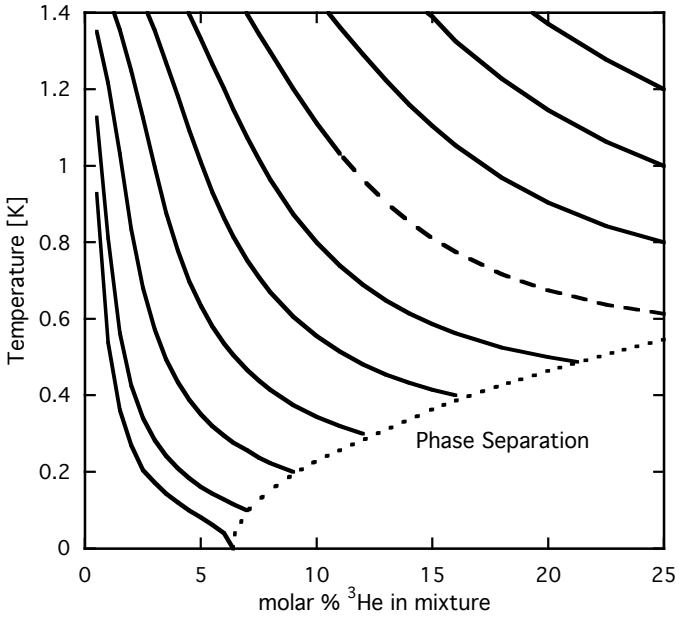

Figure C1: Selected loci of constant μ_4 for dilute ^{3}He/^{4}He mixtures. The dashed line is, approximately, the operating region of the Los Alamos PTR.

To reach the lowest temperatures limits, $x_3 \leq 0.064$. Such a pulse tube with a warm end above 0.6 K will have $x_3 < 0.01$ at the warm end and in the compressor. Such low concentrations limits the mass flow and the cooling achievable in a practical sized cooler. This type of cooler has not seen further development nor has it seen any practical application.

Currently available thermodynamic models of dilute ^{3}He in ^{4}He shows no evidence of a low temperature limit of a PTR.

D Constructing P-V and T-S Diagrams

Pressure-volume (P-V) and temperature-entropy (T-S) diagrams are constructed using the Lagrangian approach; they trace the path of a hypothetical element of gas as it moves through a system during a complete thermodynamic cycle. In a recuperative refrigerator, this can be a useful approach as a gas element passes through all of the components during a cycle. The cycle is often simplified to keep the path on curves of a constant thermodynamic parameter; e.g., isobars, isotherms, or isochors. In a PTR this approach has difficulties.[82,83]

In regenerative machines, void volumes prevent a single element from traversing the whole refrigerator during a cycle.[84] This difficulty is often overcome by assuming no void volumes in the components; e.g., heat exchangers, regenerator, compressor, and expander. When void volumes are included, some gas elements may spend a complete cycle within a single component. Each gas element follows a slightly different P-V and T-S path. All of the possible paths can be shown on the same P-V and T-S diagrams. This set of diagrams is bounded by curves similar to diagrams developed for the no-void-volume assumption. Thus, for regenerative coolers the familiar P-V and T-S diagrams can be used if they are interpreted as the envelope of the paths of all gas elements.[35]

In the small amplitude approximation, all of the thermodynamic quantities (*P*, *v*, *T*, *h*, *s*, *g*, *and m*) are sinusoidal in time. Thus, the P-V and T-S diagrams are ellipses. Traditional P-V and T-S diagrams have sharp corners. Using the small amplitude approximation will not produce diagrams with the traditional sharp corners. To maintain the sharp corners of the diagrams, the pressure waveform in the compressor can be approximated by straight lines: two isothermal legs linear in time, and two isobaric legs (Figure D1).

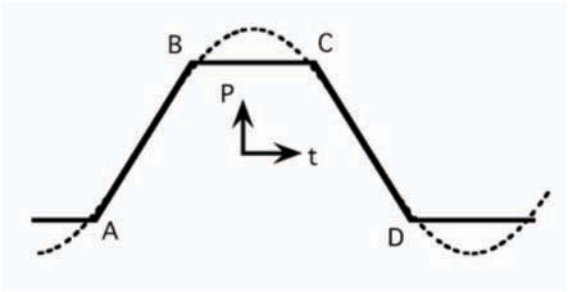

Figure D1: Solid line is the straight line approximation of the sinusoidal (dashed line) pressure oscillation.

To account for the mass flow in the pulse tube, a dimensionless parameter, Ψ, will be used. Inside the pulse tube, the flow that contributes to the cooling is in phase with the pressure and changes occur at constant volume. The volume flow in phase with the pressure at the cold heat exchanger is the same as the volume flow through the orifice. (This effect is the result of mass accumulation and is discussed in Sec. 4.3.) Since the hot heat exchanger is at higher temperature, T_h, than the cold heat exchanger, T_c, the mass flow amplitude, $\dot{m}$, for an ideal gas decreases as T^{-1} along the pulse tube. This can be characterized within the pulse tube by a dimensionless mass flow parameter:

$$\Psi = \frac{\dot{m}(T)}{\dot{m}(T_c)} = \frac{T_c}{T}. \qquad \text{(D1)}$$

Then, an entropy change, ΔS, with a mass flow, $\dot{m}(T_c)$, at the cold heat exchanger, results in a heat flow of $\dot{m}(T_c)T_c\Delta S$. At a higher temperature within the pulse tube, $\Psi T\Delta S = T_c\Delta S$. Thus, the same entropy change results in a heat flow at the hot heat exchanger of

$$\dot{m}(T_h)T_h\Delta S = \dot{m}(T_c)T_c\Delta S. \qquad \text{(D2)}$$

In the rest of the OPTR, from the cold heat exchanger to the compressor, Ψ is defined to be 1. This is equivalent to assuming that the void volumes of the regenerator and heat exchangers are small compared to the pulse tube volume. If the void volumes are included, then there is a slight gradient in Ψ in the regenerator and Figure D2 is slightly changed.

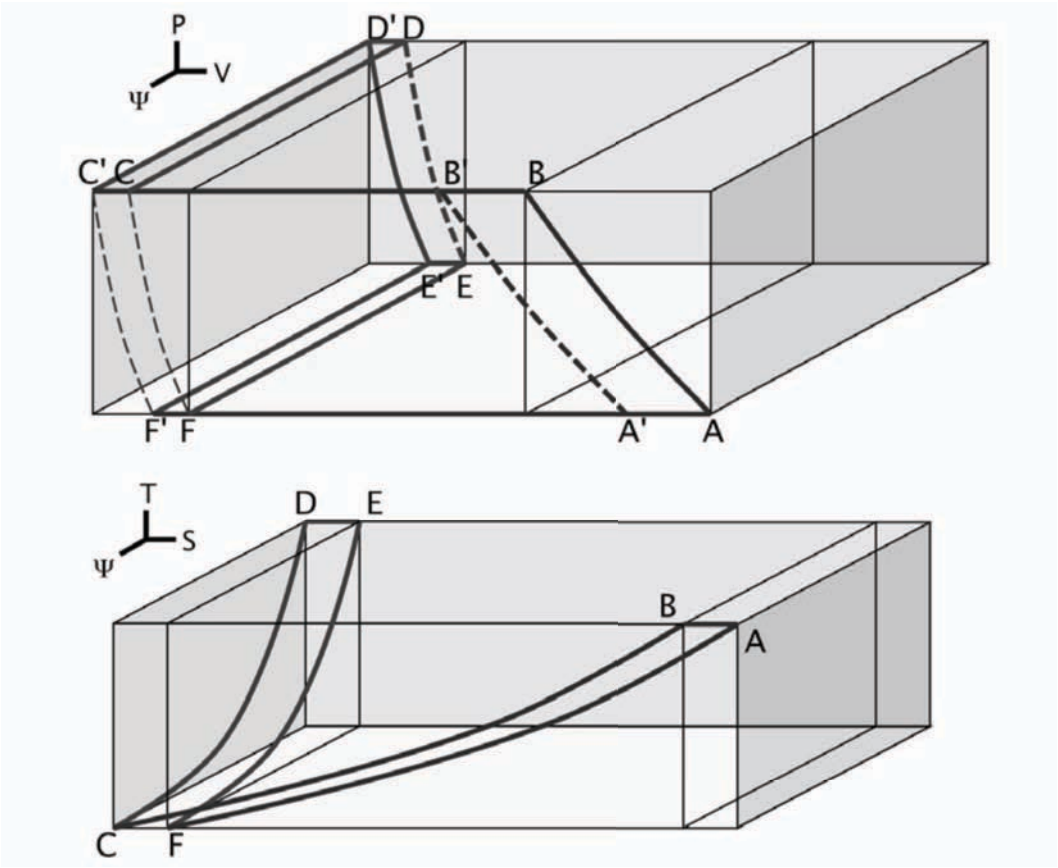

Figure D2: 3-D representation of the pulse tube cycle for an OPTR in a) P-V- and b) T-S- space. The dimensionless quantity is discussed in the text. The paths of gas elements in the compressor (A-B-C-D), the cold het exchanger (E-F-G-H), and the hot heat exchanger (I-J-K-L) are shown as solid lines. The path within the regenerator (a-b-c-d) is shown grey.

The OPTR cycle is a four-step process. We will make the same assumptions as are usually made in textbooks. The compressor, as for the Stirling cycle, is isothermal rather than adiabatic followed by an aftercooler. Figure D2 shows the paths of gas elements in the compressor, cold heat exchanger, hot heat exchanger, and regenerator as solid lines. The dashed lines connect these paths. Within the regenerator, the dashed lines correspond to a constant temperature

gradient (Sec. 4.16). Within the pulse tube, the dashed line corresponds to (D1). The pulse tube will be discussed in more detail later. The process starts at A (compressor), E (cold heat exchanger), and I (hot heat exchanger). The cycle is

a. Isothermal compression: A⇒B, E⇒F, and I⇒J. The temperatures are T_h, T_c, and T_h respectively. The pressure changes throughout the system (except for the reservoir) from $P_a - P_d$ to $P_a + P_d$. The changing pressure in the pulse tube requires mass to flow into it from the cold heat exchanger.
b. Continued displacement of the piston from B⇒C and isobaric flow through the lossless regenerator, which results in a volume flow from F⇒G at the cold heat exchanger and an equal volume flow through the orifice into the reservoir from J⇒K. The pressure remains constant at $P_a + P_d$. This is the mass flow, which contributes to the cooling.
c. Isothermal expansion: C⇒D, G⇒H, and K⇒L. The pressure changes throughout the system (except for the reservoir) from $P_a + P_d$ to $P_a - P_d$.
d. Continued displacement of the piston from D⇒A and isobaric flow through the lossless regenerator which results in a volume flow from H⇒E at the cold heat exchanger and an equal volume flows through the orifice from the reservoir from L⇒I. The pressure remains constant at $P_a - P_d$. This is the mass flow, which contributes to the cooling.

During steps 1 and 2, there is adiabatic compression and expansion, respectively, in the pulse tube. Being adiabatic, there is no direct heat transfer in the pulse tube. There is convective heat transfer at the heat exchanger to pulse tube boundary (Appendix B). The heat transfer is into the hot heat exchanger during compression and from the cold heat exchanger during expansion. For the most part, these transfers occur within the respective heat exchangers. The heat exchangers are assumed isothermal at all times. Thus, for the purposes here, all of the external heat transfers (heat and entropy flows) are considered isothermal and occur at the heat exchangers or at the compressor. This is similar to assuming, for the Stirling cycle in Figure 4, that the expansion is isothermal rather than a more realistic adiabatic piston coupled to an isothermal heat exchanger.

The compressor does work $\dot{W}$ = *path* (A-A'-B'-B-A) which is rejected as heat $\dot{W} = \dot{Q}_a = T_h \dot{S}_{AB}$. At the cold heat exchanger, expansion work = *path* (C-C'-F'-F-C) is done absorbing heat $\dot{Q}_c = T_c \dot{S}_{CF}$, where $\dot{S}_{AB} = \dot{S}_{CF}$. At the orifice, work = *path* (D-D'-E'-E-D) is dissipated and rejected as heat $\dot{Q}_h = \Psi T_h \dot{S}_{DE} = T_c \dot{S}_{DE}$, and $\dot{S}_{DE} = \dot{S}_{CF}$.

The 3-D P-V-Ψ and T-S-Ψ diagrams of Figure D2 can be projected onto 2-D P-V and ΨT-S diagrams. These are shown in Figure D3. These diagrams are similar to the P-V and T-S diagrams of the Ericsson cycle.

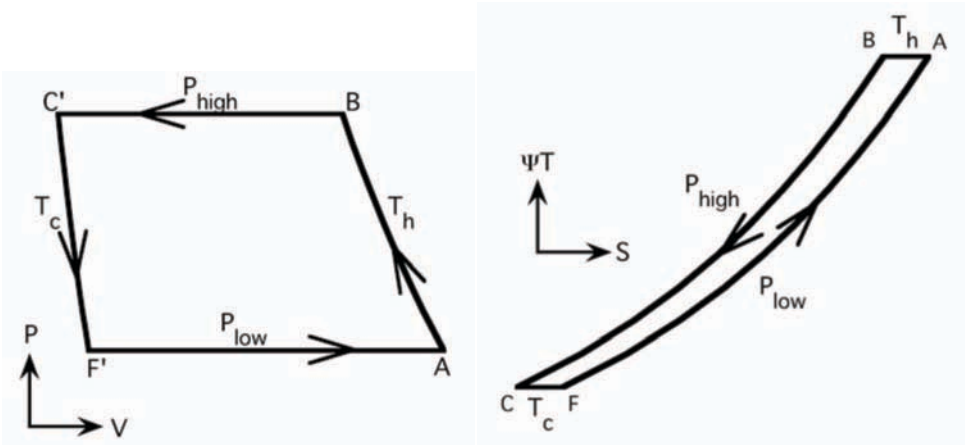

Figure D3: 2-D representation of the pulse tube cycle for an OPTR in P-V and T-S space. The dimensionless quantity is discussed in the text.

The above discussion shows that with no more idealization than used for the Stirling cycle, the OPTR refrigeration cycle can be reduced to an Ericsson cycle. The final step in this development was the suppression of the contribution of the pulse tube in Figure D3. The path of gas elements within the pulse tube was not included in Figures D2 and D3. To a certain extent, this omission is justified. The function of the pulse tube, orifice, and reservoir is to control the phase shift between the mass flow and pressure at the cold heat exchanger. They are not otherwise important to the thermodynamics of an idealized system. The principal thermodynamic components are those included in Figure D3: the compressor, regenerator, and the cold heat exchanger. The pulse tube, hot heat exchanger, and orifice form a phase shifter, as does the cold piston (or displacer) in a Stirling refrigerator.

The dotted lines used to represent P, V, T, and S in the pulse tube do not reflect the actual motion of gas elements there. The ideal pulse tube is adiabatic; i.e., the entropy of a gas element within the pulse tube is constant. This is shown by the gas element *path* (m-n) in Figure D4. Extending this over the entire pulse tube produces the envelope (M-N-O-P). There is a discontinuity between this path and the paths at the heat exchangers (F-G) and (J-K). Actually, there is no discontinuity. Rather, there is a transition region near the ends of the pulse tube. Most of the heat transfer occurs within these transitions and not in the heat exchangers (Appendix B). This is an irreversible process and not readily presented on P-V and T-S diagrams. With this limitation, presenting the OPTR cycle as an Ericsson cycle is a reasonable idealization.

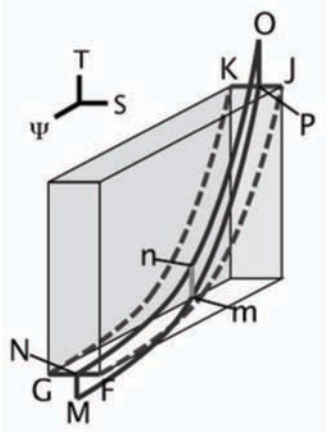

Figure D4: The T-S-Ψ diagram of the pulse tube with its two heat exchangers. Because there is less mass flow at the hot heat exchanger tan at the cold heat exchanger, path(O-P) is longer than path(M-N) – see ref. 22 for details.

E Regenerator Effectiveness/Ineffectiveness

The regenerator effectiveness is a measure of the thermodynamic quality of a regenerator. It is defined in terms heat or enthalpy transfer between the working fluid and the solid regenerator material. There is some variation in the literature of the definition.[85,86] Here, the effectiveness is defined in terms of enthalpy flows: The effectiveness, ε, is defined as the actual change in the enthalpy of the fluid to the maximum possible enthalpy transfer. The instantaneous effectiveness is

$$\varepsilon = \frac{\dot{H}_r}{\dot{H}_i} \tag{E1}$$

where $\dot{H}_r$ is the actual (real) enthalpy transfer rate and $\dot{H}_i$ is the ideal enthalpy transfer rate:

$$\dot{H}_i = \int_{T_c}^{T_h} \dot{m} c_P dT \tag{E2}$$

This is the maximum enthalpy that can be transferred from the gas to the solid material at any instant. The pressure of the gas is not the same for both flow directions. For a real gas, c_P depends on the flow direction. Thus, $\dot{H}_i$ and ε depend on the flow direction.

Here only an ideal gas is considered. For an ideal gas c_P is a constant, independent of pressure or temperature; and (E2) reduces to

$$\dot{H}_i = \dot{m} c_P (T_h - T_c) \tag{E3}$$

The instantaneous ineffectiveness is

$$1 - \varepsilon = \frac{\dot{H}_{regen}}{\dot{H}_i} \tag{E4}$$

where $\dot{H}_{regen}$ is the enthalpy flow in the regenerator; i.e., the enthalpy not transferred. As discussed in Sec. 5.7, this is the enthalpy flow in the regenerator: $\dot{m} c_P \Delta T$, where $\Delta T = \Delta T_d \sin(\omega t + \varphi_\Delta)$ is the temperature difference between the gas and solid material, as given by (5.24). The instantaneous ineffectiveness becomes:

$$1 - \varepsilon = \frac{\dot{m} c_P \Delta T_d \sin(\omega t + \varphi_\Delta)}{\dot{m} c_P (T_h - T_c)} = \frac{\Delta T_d \sin(\omega t + \varphi_\Delta)}{(T_h - T_c)} \tag{E5}$$

The average ineffectiveness is found by averaging (E5) over one flow direction, i.e. a half cycle. The average ineffectiveness becomes:

$$\langle 1 - \varepsilon \rangle = \frac{2}{\pi} \frac{\Delta T_d}{T_h - T_c} \cos(\varphi_\Delta) \tag{E6}$$

F DC Flow Losses in DPTR

The DPTR has a secondary orifice connecting the aftercooler with the hot heat exchanger. A small portion of the mass flow is diverted from the regenerator and routed through this orifice. This reduces the regenerator losses and affects the phase shift at the cold heat exchanger. Unfortunately, orifices often have asymmetrical flow impedances, resulting in a small dc flow loop through the regenerator, pulse tube, and orifice. The dc flow has been observed to cause flow and temperature instabilities[87,88,89], has been modeled[90,91], and shown to change the temperature profiles in the regenerator and pulse tube.[92] Here we will discuss the change in the temperature profile and the resulting loss. The discussion will consider the effect in the regenerator. A similar effect occurs in the pulse tube.

We will assume an ideal system, except for the dc flow and thermal conduction. There is no enthalpy flow in the regenerator due to the oscillating flow. The dc flow produces an enthalpy flow of $\dot{m}_{dc} c_P T$. In addition, there is a heat flow of $-kA\nabla T$. From the first law:

$$\dot{m}_{dc} c_P T - kA\frac{dT}{dz} = constant \tag{F1}$$

If $\dot{m}_{dc} > 0$, then the flowing mass cools as it moves along the regenerator. The heat removed increases the heat flow. Thus, ∇T becomes more negative as one approaches the cold heat exchanger.

Eq. (F1) can be integrated over the length of the regenerator, ℓ, with the boundary conditions that the ends of the regenerator are at T_h and T_c. In general, the thermal conductivity is a function of T. This may necessitate numerical integration of (F1). If k is a constant, a closed form solution exists for the regenerator:

$$T_{regen} = \left(T_c - T_h e^{\alpha\ell}\right)\left(1 - e^{\alpha z}\right)\left(1 - e^{\alpha\ell}\right)^{-1} + T_h e^{\alpha z} \tag{F2}$$

where $z = 0$ at the aftercooler end of the regenerator and $\alpha = \dot{m} c_P / kA$. For the pulse tube:

$$T_{pt} = \left(T_c - T_h e^{-\alpha\ell}\right)\left(1 - e^{\alpha z}\right)\left(1 - e^{-\alpha\ell}\right)^{-1} + T_c e^{\alpha z} \tag{F3}$$

where $z = 0$ at the cold heat exchanger end of the pulse tube. The resulting temperature profiles for (F2) and (F2) are shown in Figures F1 and F2, respectively, for a variety of values of α. The α will be different in the two components, because the k will be different. α^{-1} is a characteristic length. The deviation from the ideal temperature profile is small if $\alpha\ell \ll 1$.

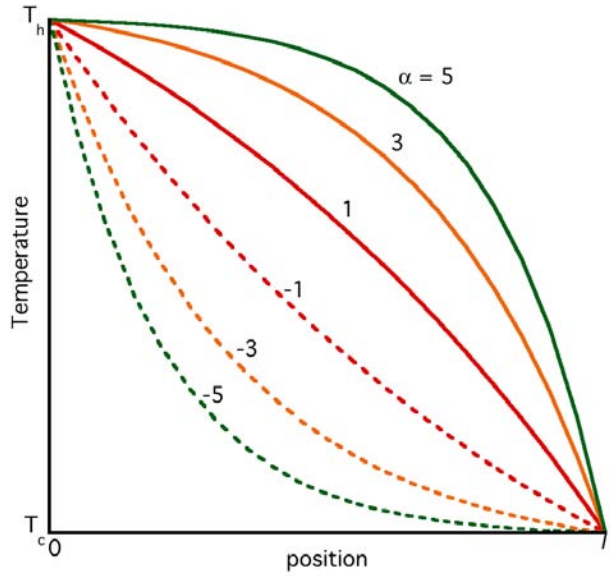

Figure F1: The temperature profile as a result of dc flow in the regenerator assuming constant *k* for a selection of flows in the positive and negative flow directions.

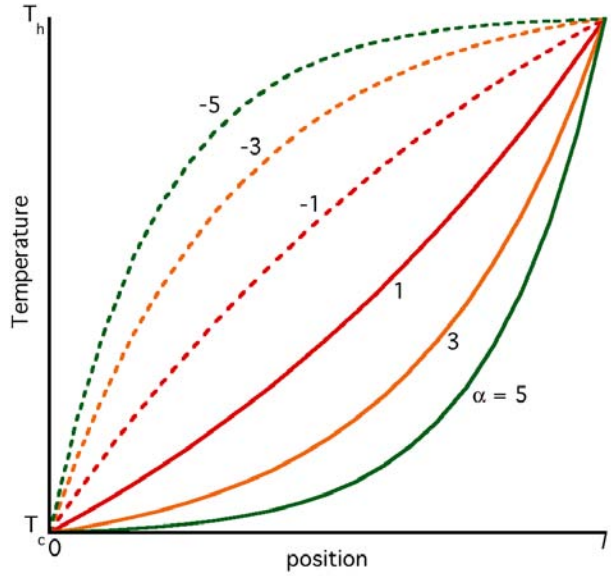

Figure F2: The temperature profile as a result of dc flow in the pulse tube assuming constant *k* for a selection of flows in the positive and negative flow directions.

The dc flow reduces the heat conduction term where the flow enters the regenerator and increases it at the exit. For the regenerator (F2), the conduction term is

$$\dot{Q}_{regen} = -k_{regen} A \frac{dT}{dz} = \dot{m}_{dc} c_P \left(T_c - T_h\right)\left(\frac{e^{\alpha z}}{1-e^{\alpha \ell}}\right) \qquad \text{(F4)}$$

and for the pulse tube (F3) the conduction term is

$$\dot{Q}_{pt} = -k_{pt} A \frac{dT}{dz} = -\dot{m}_{dc} c_P \left(T_c - T_h\right)\left(\frac{e^{\alpha z}}{1 - e^{\alpha \ell}}\right) \tag{F5}$$

Thus, the dc flow results in a net heat load on the cold heat exchanger. When the temperature dependence of *k* is included, the effect has been shown to greater for $\dot{m}_{dc}$ flowing in the direction of $\nabla T < 0$ than in the other direction.[54]

9 REFERENCES

1. R.N. Richardson, Pulse Tube Refrigeration - an Alternative Cryocooler, Cryogenics, 26, 331 (1986)

2. P.J. Storch and R. Radebaugh, Development and Experimental Test of an Analytical Model of the Orifice Pulse Tube Refrigerator, Adv. Cryo. Engin., 33, 851 (1988)

3. G.M. Harpole and C.K. Chan, Pulse Tube Cooler Modeling, Proceedings of the 6th Int. Cryocooler Conf., 1, 91 (1991)

4. S.A. Colgate, Regenerator Optimization for Stirling Cycle Refrigeration II, Proc. 8th Int. Cryocooler Conf., (1994)

5. P. C. T. de Boer, Thermodynamic Analysis of the Basic Pulse-Tube Refrigerator, Cryogenics, 34, 699 (1994)

6. J.H. Xiao, Thermoacoustic Theory for Cyclic Flow Regenerators Part I: Fundamentals, Cryogenics, 32, 895-901 (1992)

7. J.M Lee, P. Kittel, K.D. Timmerhaus and R. Radebaugh, Steady Secondary Momentum and Enthalpy Streaming in the Pulse Tube Refrigerator, Proc. 8th Int. Cryocooler Conf., (1994)

8. National Institute of Standards and Technology, math.nist.gov/~AOGallagher/auxfiles/regenstart.html

9. Gedeon Associates, sageofathers.com/

10. Los Alamos National Laboratory, www.lanl.gov/thermoacoustics/DeltaEC.html

11. ANSYS, Inc., www.fluent.com

12. Storch, PJ. and Radebaugh, R., Development and Experimental Test of an Analytical Model of the Orifice Pulse tube Refrigerator, Adv. Cryo. Eng. 33 (1988) pp. 851-859.

13. Storch, PJ., Radebaugh, R. and Zimmerman, J., Analytical Model for the Refrigeration Power of the Orifice Pulse Tube Refrigerator, Nat. Inst. of Standards and Technology, Tech Note 1343 (1990).

14. Radebaugh, R., A Review of Pulse Tube Refrigeration, Adv. Cryo. Engin. 35 (1990) pp. 1191-1205.

15. L.O. Schunk, G.F. Nellis, J.M. Pfotenhauer, "Experimental Investigation and Modeling of Inertance Tubes," J. Fluids Engin. 127 ASME (2005) pp. 1029-1037.

16. J.M. Pfotenhauer, Z.H. Gan, and R. Radebaugh, "Approximate Design Method for Single Stage Pulse Tube Refrigerators," Adv. Cryo. Engin. 53 AIP (2008) pp. 1437-1444.

17. P. Kittel, A. Kashani, J.M. Lee, and P.R. Roach: General Pulse Tube Theory, Cryogenics 36 (1996) 849-857.

18. P. Kittel: Enthalpy, Entropy, and Exergy Flows in Ideal Pulse Tube Cryocoolers, Cryocoolers 13, Springer, New York (2005) pp. 333-342.

19. P. Kittel: Enthalpy, Entropy, and Exergy Flow Losses in Pulse Tube Cryocoolers, Cryocoolers 13, Springer, New York (2005) pp. 343-352.

20. P. Kittel: Enthalpy, Entropy, and Exergy Flows – Real Gas Effects in Ideal Pulse Tube Cryocoolers, Adv. Cryo. Engin. 51, (AIP, New York, 2006) pp. 345-352.

21. P. Kittel: Performance Limits of Pulse Tube Cryocoolers Using 3He, Adv. Cryo. Engin. 53, (AIP, New York, 2008) pp. 1421-1428.

22. P. Kittel: The Role of Thermoconductivity in Pulse Tube Cryocoolers, Cryocoolers 15, (ICC Press, Boulder, 2009) pp.281-288.

23. P. Kittel: Ultimate Temperature of Pulse Tube Cryocoolers, Adv. Cryo. Engin., 55 (2010) pp. 1601-1608.

24. W.E. Gifford and R.C. Longsworth, Pulse-tube refrigeration. Trans ASME B J Eng Indust 86 (1964), p. 264-268.

25. E.I. Mikulin, A.A. Tarasov and M.P. Shrebyonock, Low-temperature expansion pulse tube. Adv Cry Eng 29 (1984), p. 629.

26. S. Zhu, P. Wu and Z. Chen, Double inlet pulse tube refrigerator–An important improvement. Cryogenics 30 (1990), p. 514-520.

27. K. Kanao, N. Watanabe, Y. Kanazawa, A miniature pulse tube refrigerator for temperatures below 100K, Cryogenics 34, Supplement 1 (1994) pp. 167-170

28. Storch, P.J., Radebaugh, R., and Zimmerman, J., Analytical Model for Refrigeration Power of the Orifice Pulse Tube Refrigerator, NIST Technical Note 1343 (1990).

29. de Waele, A.T.A.M., Steijaert, P.P., and Gijzen, P., "Thermodynamic Aspects of Pulse Tubes," Cryogenics, vol. 37 (1997) pp. 313-324.

30. de Boer, P.C.T., "Optimization of the Orifice Pulse Tube," Cryogenics, vol. 40 (2000) 701.

31. Razani, A., Flake, B., and Yarbrough, S., "Exergy Flow in Pulse Tube Refrigerators and Their Performance Evaluation Based on Exergy Analysis," Adv. Cryo. Engin., vol. 49, AIP Press, New York (2004) pp. 1508-1518.

32. J. Liang, A. Ravex and P. Rolland, Study on Pulse Tube Refrigeration Part 1: Thermodynamic Nonsymmetry Effect, Cryogenics, vol. 36, (1996) pp. 87-93.

33. J. Liang, A. Ravex and P. Rolland, Study on Pulse Tube Refrigeration Part 2: Theoretical Modeling, Cryogenics, vol. 36, (1996) pp. 95-99.

34. J. Liang, A. Ravex and P. Rolland, Study on Pulse Tube Refrigeration Part 3: Experimental Verification, Cryogenics, vol. 36, (1996) pp. 101-106.

35. J. Liang, Thermodynamic Cycles in Oscillating Flow Regenerators. J. Appl. Phys., vol. 82 (1997) pp. 4159–4165.

36. Luo E., Dai W., Radebaugh R., New Perspective on Thermodynamic Cycles of Oscillating Flow Regenerators, Proc. 20th Int. Cryo. Engin. Conf., Elsevier (2005) pp.337-340.

37. Radebaugh, R., Lewis, M.A., and Bradley, P.E., Verification of the Back-EMF Method for Piston Velocity Measurements, 17th Int. Cryocooler Conf., N. Hollywood (2012), submitted to Cryocoolers 17.

38. Black, W.Z. and Hartley, J.G., Thermodynamics, 3rd Edition, HarperCollins, New York (1996) p. 527.

39. Dai,W., and Luo, E., 2006, Clarification of Some Important Issues in Basic Thermoacoustic Theory, Adv. in Cryo. Engin. 51, edited by J. Weisend et al., AIP Press, Melville, 2006, pp. 1139-1147.

40. Kittel, P., "Ideal Orifice Pulse Tube Refrigerator Performance," Cryogenics, vol. 32 (1992) pp. 843-844.

41. Bejan, A., Advanced Engineering Thermodynamics, 2ed Edition, Wiley, New York (1997)

42. S. Zhu and Y. Matsubara, "Numerical Method of Inertance Tube Pulse Tube Refrigerator," Cryogenics 44 (2004) pp. 649-660.

43. Wang B., Wang L.Y., Zhu J.K., Chen J., Li Z.P., Gan Z.H. Study on phase shifting mechanism of inertance tube at low temperatures, presented at 17th Int. Cryocooler Conf. N. Hollywood (2012), submitted to Cryocoolers 17.

44. Lewis, M.A., Kuriyama, T., Kuriyama, F., and Radebaugh, R., "Measurement of Heat Conduction through Stacked Screens," Adv. Cryo. Engin. 43, Plenum, New York (1998), pp. 1611-1618.

45. Y. Matsubara and A. Miyake, Dept. of Atomic Energy Research Institute, Nihon U., Tokyo, Japan, Alternative Methods of the Orifice Pulse Tube Refrigerator, Proc. 5th Int. Cryocooler Conf., 127 (1989).

46. Y. Matsubara and Y. Hiresaki, Effect of Void Volume in Regenerator, Proceedings of the 6th Int. Cryocooler Conf., 1, US Navy Report, David Taylor Research Center Technical Conference Publication DTRC-91/002 (1991) pp. 173-182

47. J.M. Lee, P. Kittel, K.D. Timmerhaus, and R. Radebaugh: Flow Patterns Intrinsic to the Pulse Tube Refrigerator; Proc. 7th Int. Cryocooler Conf. (Santa Fe, NM, Nov 17-19, 1992); Philips Lab Report #PL-CP-93-1001 (1993) pp. 125.

48. Lee, JM, Steady Secondary Flows Generated by Periodic Compression and Expansion of an Ideal Gas in a Pulse Tube, Ph.D. Thesis, University of Colorado at Boulder (1997).

49. J.R. Olson and G.W. Swift, Cryocoolers, Suppression of Acoustic Streaming in Tapered Pulse Tubes, Vol. 10, Plenum Press (1998) pp. 307-314.

50. G.W. Swift, M.S. Allen, and J.J. Wollan, Performance of a Tapered Pulse Tube, Cryocoolers, Vol. 10, Plenum Press (1998) pp. 315-320.

51. Cha, J.S., Ghiaasiaan, S.M., Kirkconnell, C.S., and Clearman, W.M., "The Impact of Uncertainties Associated with Regenerator Hydrodynamic Closure Parameters on the Performance of Inertance Tube Pulse Tube Cryocoolers," Adv. Cryo. Engin., vol. 53, AIP Press, New York (2008) 243-250.

52. D.Gedeon, Flow Circulations in Foil-Type Regenerators Produced by Non-Uniform Layer Spacing, Cryocoolers 13 (2004) pp. 421-430.

53. M. Dietrich, L.W. Yang, G. Thummes, High-Power Stirling-Type Pulse Tube Cryocooler: Observation and Reduction of Regenerator Temperature-Inhomogeneities, Cryogenics, vol. 47 (2007) pp. 306–314.

54. L.M. Qiu, J.C. Sun, M. Dietrich, G. Thummes, Z.H. Gan, Flow Circulations Produce by Non-Uniform Porosity in the Regenerator of High Power Pulse Tube Cryocooler, in preparation.

55. Yuan Yuan, Zhi Xiaoqin, He Wei, Gan Zhihua, Qiu Limin, CFD simulation and experimental study on the optimum expansion volume of a pulse tube operating in the hundred Hz Range, presented at 17th Int. Cryocooler Conf., N. Hollywood (2012), submitted to Cryocoolers 17.

56. L.M. Qiu, T. Numazawa, G. Thummes, Performance Improvement of a Pulse Tube Cooler Below 4 K by Use of GdAlO3 Regenerator Material, Cryogenics, vol. 41 (2001) pp. 693-696.

57. N. Jiang, U. Lindemann, F. Giebeler, G. Thummes, A 3He Pulse Tube Cooler Operating Down to 1.3 K, Cryogenics, vol. 44 (2004) pp. 809–816

58. J.R. Olson, M. Moore, P. Champagne, E. Roth, B. Evtimov, J. Jensen,A. Collaco, and T. Nast, Development of a Space-Type 4-Stage Pulse Tube Cryocooler for Very Low Temperature, Adv. Cryo. Engin. 51 edited by J. Weisend et al., AIP Press, Melville, 2006, pp. 623-631.

59. T. Nast, J. Olson, P. Champagne, J. Mix, B. Evtimov, E. Roth, and A. Collaco, Development of a 4.5 K Pulse Tube Cryocooler for Superconducting Electronics, Adv. Cryo. Engin. 53 edited by J. Weisend et al., AIP Press, Melville, 2008, pp. 881-886.

60. HE3PAK v1.2 and HEPAK v3.4, available from Horizon Technologies, Littleton, CO, USA.

61. Arp, V., Preliminary version of HEPAK v4, private communication, Aug 2008.

62. Radebaugh, R., Lewis, M., Luo, E., Pfotenhauer, J. M., Nellis, G. F., and Schunk, L. A., "Inertance Tube Optimization for Pulse Tube Refrigerators," in Advances in Cryogenic Engineering 51, edited by J. Weisend et al., AIP Press, Melville, 2006, pp. 59-67.

63. Esel'son, B.N., Grigor'ev, V.N., Ivantsov, V.G., Rudavskii, E.Ya., Sanikadze, D.G., and Serbin, I.A., Solutions of He3 - He4 Quantum Liquids, Nauka, Moscow, 1973 (in Russian) p. 424.

64. Ebner, C. and Edwards, D.O., Physics Reports 2, pp. 77-154 (1971).

65. B.J. Huang, L.T. Lee and C.W. Lu, System Design Analysis of Pulse-Tube Cryocooler, Proceedings of the 6th Int. Cryocooler Conf., 1, US Navy Report, David Taylor Research Center Technical Conference Publication DTRC-91/002 (1991) pp. 77-90.

66. Roach. P.R., private communication, formally available at http://irtek.arc.nasa.gov/CryoGroup/PTDatabase/PTData-Basic.htm

67. Lechner, R.A., and Ackerman, R.A., "Concentric Pulse Tube Analysis and Design," Adv. Cryo. Engin. 18, Plenum, New York (1973) pp. 467-474.

68. K.G. Narayankhedkar and V.D. Mane, Investigation of Pulse Tube Refrigerator, J. of Engineering for Industry, 373 (Feb. 1973).

69. M. David and C.-C. Marechal, An Experimental Investigation of Pulse Tube Refrigeration Heat Transfer Rates, Adv. Cryo. Engin., 35, 1231 (1990).

70. Y. Matsubara and A. Miyake, Alternative Methods of the Orifice Pulse Tube Refrigerator, Proc. 5th Int. Cryocooler Conf., 127 (1989).

71. R.N. Richardson, Institute of Cryogenics, Development of a Practical Pulse Tube Refrigerator: Coaxial designs and the Influence of Viscosity, Cryogenics, 28, 516 (1988).

72. R.A. Lechner and R.A. Ackermann, Concentric Pulse Tube Analysis and Design, Adv. Cryo. Engin., 18, 467 (1973).

73. Richard A. Lechner, Investigation of Regenerators and Pulse Tube Cryogenic Coolers, Technical Report, ECOM-3409.

74. R. C. Longsworth, An Experimental Investigation of Pulse Tube Refrigeration Heat Pumping Rates, Adv. Cryo. Engin., 12, 608 (1967).

75. W.E. Gifford and G.H. Kyanka, Reversible Pulse Tube Refrigeration, Adv. Cryo. Engin., 12, 619 (1967).

76. W. E. Gifford and R. C. Longsworth, Pulse Tube Refrigeration Progress, Adv. Cryo. Engin., 10B, 69 (1965).

77. Kar, K., Dadd, M.W., Bailey, P.B., and Stone, C.R., "Fast Response Temperature Measurements in Stirling Cycle Cryocooler Components," Adv. Cryo. Engin. 53, AIP Press, Melville (2008), pp. 1675-1682.

78. Radebaugh, R., Thermodynamic Properties of He3-He4 Solutions with Applications to the He3-He4 Dilution Refrigerator, NBS TN 362 (1967), available from NTIS (www.ntis.gov).

79. Kuerten, J.G.M. , Castelijns, C.A.M. , de Waale, A.T.A.M. , and Gijsman, H.M., Cryogenics 24, pp. 419-443 (1985).

80. Chaudhry, G. and Brisson, J.G., "Thermodynamic properties of 3He-4He mixtures between 0.15 K and 1.8 K," Adv. Cryo. Engin., 55 (2010) pp. 1562-1569 and J. Low Temp. Phys., 158 (2010) pp. 806-853.

81. Watanabe, A., Swift, G.W., and Brisson, J.G., "Superfluid Orifice Pulse Tube Refrigerator below 1 Kelvin," in Adv. in Cryo. Engin. 41, edited by P. Kittel, Plenum Press, New York, 1996, pp. 1519-1526.

82. P. Kittel: Are P-V and T-S Diagrams Meaningful for Regenerative Cryocoolers?, Cryocoolers 16 (2011) pp.437-443.

83. P. Kittel: Constructing P-V and T-S Diagrams for Pulse Tube Refrigerators, Proc. 23rd Int. Cryogenic Engin. Conf. (ICEC 23), Wroclaw University of Technology (2011) pp. 205-210.

84. Luo, E., Dai, W., and Radebaugh, R., New perspective on thermodynamic cycles of oscillating flow regenerators, Proc. 20th Int. Cryogenic Engineering Conf. (ICEC 20) Elsevier, Oxford, UK (2005) pp. 337-340.

85. D.E. Daney, Regenerator Performance with Sinusoidal Flow, Cryogenics, 31 (1991) pp. 839-841.

86. G.F. Nellis, A Heat Exchanger Model that Includes Axial Conduction, Parasitic Heat Loads, and Property Variations, Cryogenics, 43 (2003) pp. 43-538.

87. T. Shigi, Y Fujii, M. Yamamoto, M. Nakamura, M. Yamaguchi, Y. Fujii, T. Nishitami, T Araki, E. Kawaguchi, and M Yanai, Anomaly of One-Stage Double-Inlet Pulse Tube Refrigerator, Proc. 16th Int. Cryo. Engin. Conf., Elsevier, (1997) pp. 263-266.

88. N. Seki, S. Yamasaki, J. Yuyama, M. Kasuya, K, Arasawa, S. Furuya, and H. Morimoto, Temperature stability of Pulse Tube Refrigerators. Proc. 16th Int. Cryo. Engin. Conf. (ICEC 16), Elsevier, (1997) pp. 267-270.

89. C. Wang, G. Thummes and C. Heiden, Effects of DC Gas Flow on Performance of Two-Stage 4 K Pulse Tube Coolers, Cryogenics, 38, (1998) pp. 689-695.

90. D. Gedeon, DC Gas Flow in Stirling and Pulse Tube Cryocoolers, Cryocoolers 9, Plenum Press, (1997) pp. 385-392.

91. L. Yang, Y. Zhou, J. Liang, DC Flow Analysis and Second Orifice Version Pulse Tube Refrigerator, Cryogenics, 39, (1999) pp. 187-192.

92. L. Duband, L. Charles, A. Ravex, L. Miquet, and C. Jewell, Experimental Results on Inertance and Permanent Flow in Pulse Tube Coolers, Cryocoolers 10, Plenum Press, (1999) pp. 281-290.